A Computational Study on the Ca^{2+} Solvation, Coordination Environment, and Mobility in Electrolytes for Calcium Ion Batteries

Saeid Biria,[1] Shreyas Pathreeker,[1] Ian D. Hosein[1*]

1. Syracuse University, Department of Biomedical and Chemical Engineering, Syracuse, NY, 13244

Correspondence: idhosein@syr.edu

ABSTRACT

Calcium (ion) batteries are promising next-generation energy storage systems, owing to their numerous benefits in terms of performance metrics, low-cost, mineral abundance, and economic sustainability. A central and critical area to the advancement of the technology is the development of suitable eletrolytes that allow for good salt solubility, ion mobility, electrochemical stability, and reversible redox activity. At this time, the study of different solvent-salt combinations is very limited. Here, we present a computational study on the coordination environment, solvation energetics, and diffusivity of calcium ions over a range of pertinent ionic liquids, cyclic and acylic alkyl carbonates, and specific alkyl nitriles and alkyl formamides, using the salts calcium bis(trifluoromethylsulfonyl)imide ($Ca(TFSI)_2$) and calcium perchlorate ($Ca(ClO_4)_2$). Key findings are that several solvents from different solvent classes present comparable solvation environments and mobilities. $Ca(TFSI)_2$ is prefered over $Ca(ClO_4)_2$ owing to the former's mix coordination of Ca^{2+} to O and N atoms. Ionic liquids with alkyl sulfonate anions provide better coordation over TFSI, which leads to greater diffusivity. Binary organic mixtures (carbonates) provide the best solvation of Ca^{2+}, however, single organic solvents also provide good solvation, such as EC, THF and DMF, as well as some acyclic carbonates. Ion pairing with the salt anion is always present, but can be mitigated through solvent selection, which also correlates to greater mobility; however, there are examples in which strong ion pairing is not significantly adverse to diffusivity. The solvent incorporate into the solvation structure with binary organic mixtures correlates well with the solvation capabilities of the individual solvents. Finally, we show that ionic liquids (specifically alkyl imidazole (cation) alkyl sulfonate (anion) ionic liquids) do not decompose when coordinating at a Ca metal interface, which indicates its promising stability. Overall, this study contributes further generalized understanding of the correlation between solvent and salt and the resultant Ca^{2+} complexes and Ca^{2+} mobility in a range of electrolytes, and reveals a range of possible solvents suitable for exploration in calcium (ion) batteries.

KEYWORDS

Calcium batteries, ionic liquids, electrolytes, molecular dynamics simulations, energy

1. INTRODUCTION

Calcium (ion) batteries have emerged as potential next-generation electrochemical energy storage systems.[1-4] As examples of their benefits, calcium is the most abundant alkaline earth element and the 5th most abundant element in the Earth's crust. Ca sourcing is low-cost and of significant global production (e.g., crushed lime) to supply its future battery industry. Electrochemically, based on standard reduction potentials, calcium can have a similar cell potential as lithium, and greater than magnesium and sodium. Kinetically, owing to calcium's larger ionic radius (1.00 Å) than magnesium (0.72 Å), which is also similar to Na (1.02 Å), Ca^{2+} may have faster diffusion in electrolytes due lower charge density and polarizing properties. There is particular interest in the development of calcium metal batteries,[1, 4-6] owing to its potential to achieve similar performance figure of merits as incumbent Li-ion technology.[7]

A crucial bottleneck to developing rechargeable Ca metal batteries is the lack of suitable electrolytes,[8-9] as has been the case for many multivalent systems,[10] that can simultaneously satisfy conditions such as : i) exhibit high ionic conductivity and transference number, both of which depend upon the solubility of the salt in the solvent, ii) allow facile desolvation of solvated cations ions in a reversible manner, which is connected to the nature of the salt anion, extent of ion-pairing, and stability of the coordinated complexes, iii) possess a wide electrochemical stability window, and iv) must be stable against metallic calcium to minimize side reactions and decomposition. Challenges meeting the above conditions are in part owing to the unique solvation and solubility properties of divalent ions, entailing strong coordination to its environment (be it through ion pairing or solvation) as well as the strong reducing nature of multivalent metals. Thus far, studies that have elicited Ca redox activity or proposed Ca battery architectures have explored electrolytes composed of solvents such as alkyl carbonates (e.g., EC, PC),[11-13] THF,[14] DME,[15-16] ionic liquids,[17-19], and glymes.[20-21] Salts that have been explored with these solvents have included $Ca(BF_4)_2$, $Ca(TFSI)_2$, $Ca(TFS)_2$, $Ca(ClO_4)_2$, $Ca(BH_4)_2$, $Ca[B(hfip)_4]_2$, as well as $Ca(PF_6)_2$.[22-23] Mixed cation salts (Ca+Li or Ca+Na) in carbonate or THF solvents have also been proposed towards engineering the solid electrolyte interface (SEI),[24-25] namely the solid layer formed at the electrode/electrolyte interface from the decomposition of electrolyte (both solvent and salt) and is permeable to ions to allow for redox activity to proceed. Additionally, a range of commercial salts have been examined experimentally for their solvation properties in solvents such as PC, EC, DMF, THF, DME, and glymes.[26-27]

Theoretical predictions have impactfully contributed to understanding of calcium electrolytes, particularly in revealing the solvation environment, energetics, and predicted decomposition products; however, such studied remain at nascent levels. Thus far, studies have included elucidating solvation environments when employing cyclic and acyclic carbonates with $Ca(BF_4)_2$ and glymes with $Ca(TFSI)_2$,[21, 28] screening of solvent molecules,[29] simulating EC decomposition at a Ca metal interface,[30-31] ionic liquid coordinated

crystal structures,[18] as well as properties of aqueous solutions.[32] Yet, there remains a lack of computational studies that comparatively explore a range of different solvent classes/types and salt compositions. Additionally, specific correlations between solvation and particularly Ca^{2+} mobility (i.e., diffusivity) remain a gap in understanding. All solvents thus far explored experimentally have been done so owing to some favorable properties: Alkyl carbonate electrolytes are good solvents for a range of calcium salts.[26] Ionic liquids are well known for their good solubility, mobility, and electrochemical stability.[17, 33] Other non-carbonates yield good electrolyte properties in calcium ion batteries.[26, 34] Yet, as is the case for many of them, such as acetonitrile,[34-36] THF[24] and DMF,[26] complimentary theoretical studies are lacking. $Ca(TFSI)_2$ and $Ca(ClO_4)_2$ are also understudied, despite the former showing one of the highest conductivities for the explored calcium salts and having been employed in battery studies,[26, 35, 37] and the latter appears to have been overlooked, perhaps owing to the low plating/stripping kinetics.[12] Only a brief study of the solvation of $Ca(ClO_4)_2$ in EC was performed, but in the broader context of exploring the decomposition of alkyl carbonate solvents at a calcium metal interface.[30]

Overall, the selective and somewhat sparse nature of existing reports on electrolytes prompts the probing of a more encompassing study of Ca^{2+} solvation, which can be easier to achieve with computational tools compared with experimental efforts. Furthermore, the choice of these electrolytes has thus far been empirical, often drawing from Li and Mg equivalents, since there are no reported theoretical studies to provide a systematic comparison over a range of different solvent-salt systems to identify ideal electrolytes that can influence the overall performance of the calcium ion batteries. Hence, a cross-cutting solvent-salt study is needed to help provide broader, comparative understanding and generalized principles of the Ca^{2+} solvation in candidate electrolytes. Hence, the work herein aims to contribute to the understanding of calcium ion electrolytes by exploring in a more expansive range of alkyl carbonate, ionic liquid, alkyl nitrile, alkyl formamide, and ether based solvents combined with either $Ca(TFSI)_2$ or $Ca(ClO_4)_2$. The studies are carried out by conducting molecular dynamics (MD) simulations, DFT-based ab initio calculations, and ab initio molecular dynamics (AIMD) simulations.

2. COMPUTATIONAL METHODS

2.1. Systems

The simulated environment consisted of the selected solvents with either $Ca(TFSI)_2$ or $Ca(ClO_4)_2$ to form model electrolytes. The number of salt and solvent molecules was set so as to emulate an approximate 1 M concentratoin. The ionic liquids examined here in were: 1-ethyl-3-methylimidazolium trifluoromethanesulfonate ([EMIM][Otf]), 1-butyl-1-methylpyrrolidinium bis(trifluoromethylsulfonyl)imide ([BMP][TFSI]), 1-ethyl-3-methylimidazolium bis(trifluoromethylsulfonyl)imide ([EMIM][TFSI]), 1-hexyl-3-methylimidazolium chloride

([HMIM][Cl]), 1-ethyl-3-methylimidazolium methanesulfonate ([EMIM][$MESO_3$]), 1-butyl-3-methylimidazolium trifluoromethanesulfonate ([BMIM][Otf]). These ionic liquids were selected owing to their commercial availability or previous use with Ca or other electrolyte systems.[17] The organic solvents examined here in were: acrylonitrile (AC), diethyl carbonate (DEC), dimethyl carbonate (DMC), dimethylformamide (DMF), ethylene carbonate (EC), ethylene methyl carbonate (EMC), propylene carbonate (PC), vinylene carbonate (VC), and tetrahydrofuran (THF). Images of their chemical structures, for reference, are shown in **Figure 1**. The two salts were selected based on their commercial availability, high solubility, and use in previous experimental work.[2, 35-36] $Ca(BF_4)_2$ has been excluded from our studies owing to its decomposition products being impermeable to calcium owing to CaF_2 and carboxylates,[12] and its examination previously.[28] The solvents and their classes have been shown to be stable in previous theoretical and experimental work.[12, 14, 29] Molecular dynamics simulations and density functional theory calculations using the Vienna ab initio simulation package (VASP)[38] were performed within the commercial MedeA® software.

In terms of selection of system size, the ratio of salt molecules to solvent we set to have an ~1M concentration in the system. Moelcular dynamics simulations were set to have 10 salt molecules, and the number of solvent molecules adjusted accordingly. In the density functional calculations, 1 salt molecule was examined, and once again the number of solvent molecules adjusted accordingly. Hence, in the LAMMPS simulations this gave systems with 10 salt molecules and 33-60, 82-190, and 32-67 solvent molecules for ILs, single organic, and binary organic solvents, respectively. Likewise, in VASP simulations there was 1 salt molecule and 3-6, 8-19, and 3-7 molecules for ILs, single organic, and binary organic solvents, respectively. Simulation size (box size) was 25 × 25 × 25 Å. A summary of the solvent dielectric constants and the number of molecules used in each simulation are provided in **Tables S1** and **S2**, respectively.

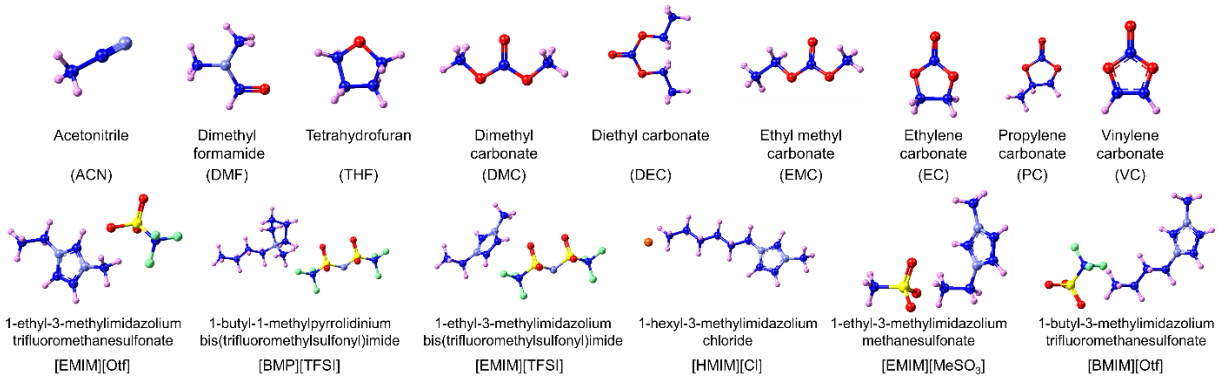

Figure 1. Summary of solvent molecules and their abbreviations. Color legend: Blue, Carbon; Red, Oxygen; Light Purple, Hydrogen; Yellow, Sulfur; Light Blue, Nitrogen; Light Green, Fluorine; Orange, Chlorine.

2.2. Molecular Dynamics Simulations

Molecular dynamic simulations for diffusion and radial distribution functions (RDFs) were performed using a Large-scale Atomic/Molecular Massively Parallel Simulator (LAMMPS),[39] using pcff+ force fields. The pcff+ force fields have been used to simulate ionic liquids with some lower accuracy,[40] but was found sufficient herein for comparsion among the solvents. The initial configurations were created in a cell consisting of a mixture of calcium salt and each solvent, followed by structure minimization and equilibration.[41-42] All MD simulations were performed using the LAMMPS code. During initialization, 3D periodic boundary conditions were applied to the system, and long-range Coulombic interactions were calculated using the particle− particle−particle−mesh (PPPM) method with the nonbonding cutoff set to 9.5 Å and the long-range precision set to 0.00001. Tail corrections were applied using Van der Waals interactions. The first equilibration step was carried out using a minimization step with conjugate gradients, followed by a classical 100 ps NPT ensemble with a timestep of 1 fs and isotropic constraint, in accordance to previous methods.[40] The Nose–Hoover thermostat was used with a temperature damping of 100 fs, and a pressure damping of 100 fs. The third and final equilibration step using classical MD was carried out using 100 ps NVT dynamics, also with a timestep of 1 fs and the Nose–Hoover thermostat with a temperature damping of 100 ps. The self-diffusion coefficient of the calcium ion salts in the solvent electrolytes was obtained by calculation of its mean squared displacement (MSD) over 10 ns over a temperature range of 273.15 to 373.17 K. Diffusion coefficients were determined based on the Einstein diffusion equation, using the MedeA Diffusion package, based on the MSD of Ca^{2+} over 10 ps (See **Figure S1-S3**). The structural characteristics of electrolytes were analyzed for different atom pairs by calculating RDF determined from MD simulation trajectories.

2.3. Density Functional Theory Calculations

The density functional theory (DFT) calculations were conducted with the automated choice projector method and the exchange-correlation functional of Perdew-Berke-Ernzerh functional of generalized gradient approximation (GGA-PBE).[39, 43] The plane-wave cutoff energy was chosen 400 eV and a 1×1×1 k-point grid for all of the calculations. The solvation energies of a single calcium salt molecule dissolved in each solvent was performed at salt:solvent molecule ratios to mimic an ~1 M concentration, and were obtained by the difference between the Gibbs free energy before and after applying the dielectric constant of each solvent (Table S1) using DFT-MD as implemented in VASP. Binary component solvents were always present in equimolar quantities (i.e., same number of molecules in the simulation). Specifically, the solvation energies were obtained via the difference between VASP GBE–PBE correlations with and without

application of the dielectric constant using the implicit solvent model.[44] In the model, the free energy of solvation ($\Delta E_{solvation}$) is calculated by subtracting the electronic energy of the solvent molecule in vacuum ($E_{continuum}$) from the electronic energy of the solvent molecule in a dielectric continuum ($E_{continuum}$) (by applying the dielectric constant of the solvent to the box):

$$\Delta E_{solvation} = E_{continuum} - E_{vacuum} \quad (1)$$

2.4. Ab Initio Molecular Dynamics Simulations

The reductive breakdown characteristics of solvent [EMIM][Otf] was investigated using AIMD simulations up to 5000 fs (with a time step of 2 fs). First, a box of 6 [EMIM][Otf] molecules was first equilibrated to its target density of 1.26 g/mL, and then merged with an optimized 3×2×1 calcium metal surface ([001]-terminated) to model the solvent–Ca-metal interface. Molecular dynamics (MD) simulations were performed using the canonical ensemble (nVT) with a planewave cutoff energy of 300 eV and convergence of 10^{-6} eV using the blocked Davidson algorithm. Gaussian smearing with a width of 0.05 eV was used as was a k-spacing of 1/Å, i.e., the gamma-point, which led to a mesh size of 1×1×1. This simulation was performed under 0 V conditions.

3. RESULTS AND DISCUSSION

To navigate the extensive data provided herein, we first present the radial probabilites of atoms in coordination to Ca^{2+}. We then discuss the structure Ca^{2+} complexes and account for their composition. Calculations of their solvation energies are reported, then diffusivity data and a discussion of correlations to Ca^{2+} complex structure. AIMD data of ionic liquid stability at a Ca interface is finally reported. Data for electroltyes with $Ca(TFSI)_2$ are showin the manuscript, and unless otherwise presented, and corresponding data for electrolytes with $Ca(ClO_4)_2$ are provided in the Supporting Information.

3.1. Coordination Environment

Figure 2-4 show RDFs, g(r), for the distance correlation between Ca^{2+} and other likely coordinating atoms from the salt or solvent. The radial distribution functions reveal much information about the solvation structure and composition environment, and their variations with solvent and salt. Beginning with ionic liquids (Figure 2), the RDF profiles show that Ca^{2+} interacts most strongly with nitrogen as well as the oxygen from the sulfonate (S=O). The probability of either the N and O atom in the first solvation shell is higher than for any other atom. Two exceptions are [EMIM][TFSI] in which the N and F from the $TFSI^-$ anion (both from the IL and the calcium salt) defines the solvation shell size, and [HMIM][Cl] in which chlorine is present with greater probability. [EMIM][TFSI] has an anomalous RDF profile relative to other IL solvents, however, replicate simulations showed the profile was consistent (Figure S4), with N from

TFSI defining the first solvation shell, and no evident first peak. [EMIM][MESO3] and [BMIM][Otf] primarily show probability for O. The distances which define the size of the first solvation shell and the atom which defines it are: 2.42 (N), 2.42 (N), 3.75 (N/F), 2.70 (N), 2.42 (N), and 2.42 (N) (O) Å for [EMIM][Otf], [BMP][TFSI], [EMIM][TFSI]), [HMIM][Cl], [EMIM][$MESO_3$], [BMIM][Otf], respectively. The differences between [BMP][TFSI] and [EMIM][TFSI], despite both having that same anion common with the salt anion (TFSI), may be owing to the difference with the IL cation. Their RDF profiles do not discern the source of the S=O bond as either from salt or solvent anion owing to having the same anion (TFSI), as is also the case for [EMIM][Otf], [EMIM][MESO3], and [BMIM][Otf] which have sulfonate groups in common. This is considered in the examination of the solvated structures to account for anion contributions from the salt and solvent (See Section 3.2). With regards to the ionic liquids with $Ca(ClO_4)_2$, the RDFs (Figure S5) show probability of coordination with the oxygen from the perchlorate. [EMIM][Otf], [BMP][TFSI], [EMIM][TFSI], and [BMIM][Otf] show probability of coordination with the sulfonate of the IL anion, [HMIM][Cl] being an exception because of the IL's anion Cl^-, and interestingly [EMIM][MESO3] shows little probability of coordination with a sulfonate. These results indicate an overall greater presence of O in the solvation shell, most likely owing to the stronger coordination of the perchlorate, and in turn the greater coordination with the O in ILs from TFSI or sulfonate-based anions.

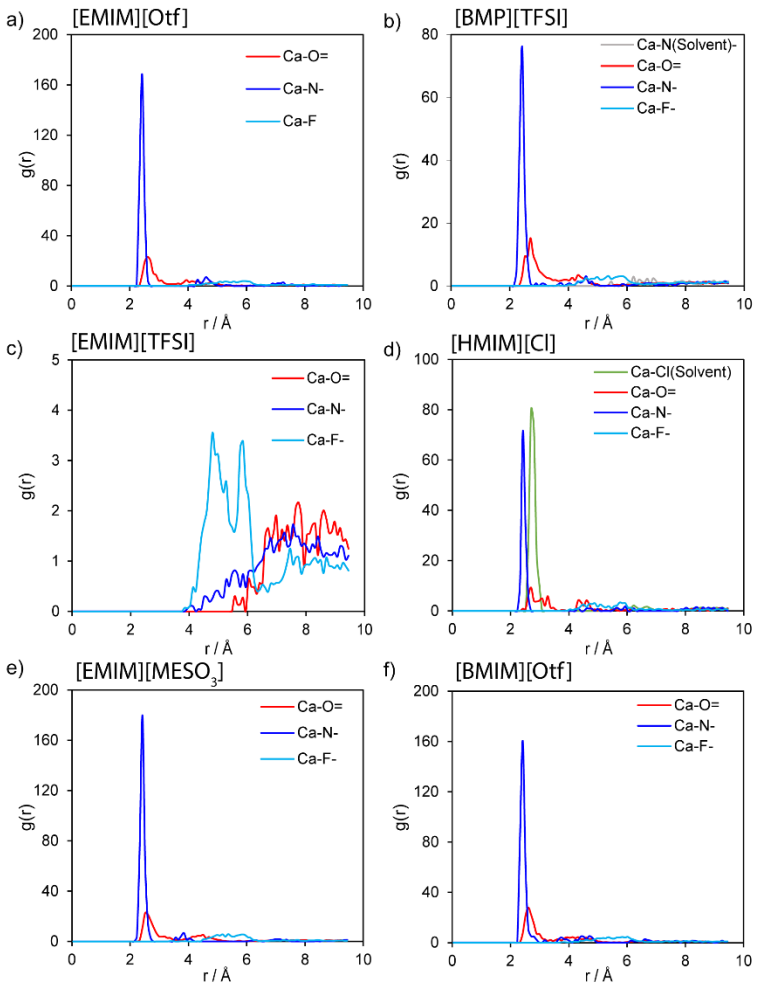

Figure 2. Radial distribution functions for electrolytes with ionic liquid solvents and $Ca(TFSI)_2$. Ionic liquid solvents show are (a-f) [EMIM][Otf], [BMP][TFSI], [EMIM][TFSI], [HMIM][Cl], [EMIM][MESO3], [BMIM][Otf], respectively. Legend entries are of the form Ca-X(bond), where X is the coordinating atom, "bond" is how the coordinating atom is bonded to its molecule (single "-" or double bond "="), with Cl being an exception. Plots are shown for all possible coordinating atoms, which are O, N, F, and Cl. When it was possible to distinguish, the label "Solvent" is used to indicate coordinating atoms from the solvent molecules, in this case the IL anion $TFSI^-$, to distinguish atoms of the same element from the salt anion. The RDFs indicate that O and N from either TFSI or IL anion (which are the same in [BMP][TFSI], [EMIM][TFSI]) are the primary coordinating atoms in the first solvation shell.

Examining the RDFs for single organic solvents (Figure 3), the first solvation shell has shared probability of the presence of an O atom from either the carbonate or ether of the solvent or the O or N atom from the TFSI. ACN is an exception, owing to its coordinating N (from C≡N), and the solvation shell shares probability of both N (solvent) and O (from TFSI). For DMF, there is significant probability of the N from TFSI and to a lesser extent. the carbonyl from DMF. THF has greater probability of the N and even F from

TFSI than the ether from THF DMC, DEC, EMC and PC all have similar probabilities for the O from C=O (first peak) from the solvent molecule and relatively greater probability of N from the TFSI (second peak), with O from TFSI present but very low relatively (weaker third peak). In EC, the O from C=O presents a greater probability (and first peak) following by the N of TFSI, and to a lesser degree the O from TFSI. For VC, the greatest probability is the N from TFSI (first peak), followed weakly by the O atom of TFSI. Considering their atom probabilities and positions, the size of the first solvation shell (determined by the position of the first peak in the RDF) is defined by the solvent for DMC, DEC, EMC, EC, and PC; all others (ACN, DMF, THF, VC) have the first solvation shell defined by the salt anion. The position of the first peak for ACN, DMF, THF, DMC, DEC, EMC, EC, PC, and VC are 2.42 (N), 2.42 (N), 2.32 (F), 2.23 (O), 2.23 (O), 2.23 (O), 2.23 (O), 2.32 (O), 2.42 (N) Å. It should be noted that solvent and salt atom probabilities peaks in proximity and relatively significant probability will present themselves in the solvated structure, as is the case with DMC, DEC, EMC and PC (See Section 3.2), whose O from C=O of the solvent molecule is followed closely by the N of TFSI. With regards to the single organic solvents with $Ca(ClO_4)_2$, the RDFs (Figure S6) generally show strong probability of coordination with the O/N for the solvent and the O from the perchlorate. All carbonates (DMC, DEC, EMC, EC, PC) have greater probability (first peak) from the O of their C=O group. VC shows similar probability and close peaks with the O from the perchlorate. DMF, THF shows greater probability of O from the perchlorate, but at approximately the same position for both peaks. ACN shows the first peak from the O from perchlorate, followed closely by the N from the C≡N group. The RDFs are comparable to those with $Ca(TFSI)_2$, in that, for example, the carbonate solvents can displace the salt anion. Yet owing to the lower probability of the O from ClO_4 (second peak following the O from the carbonates in the RDFs), it appears that ClO_4^- is more easily displaced than $TFSI^-$.

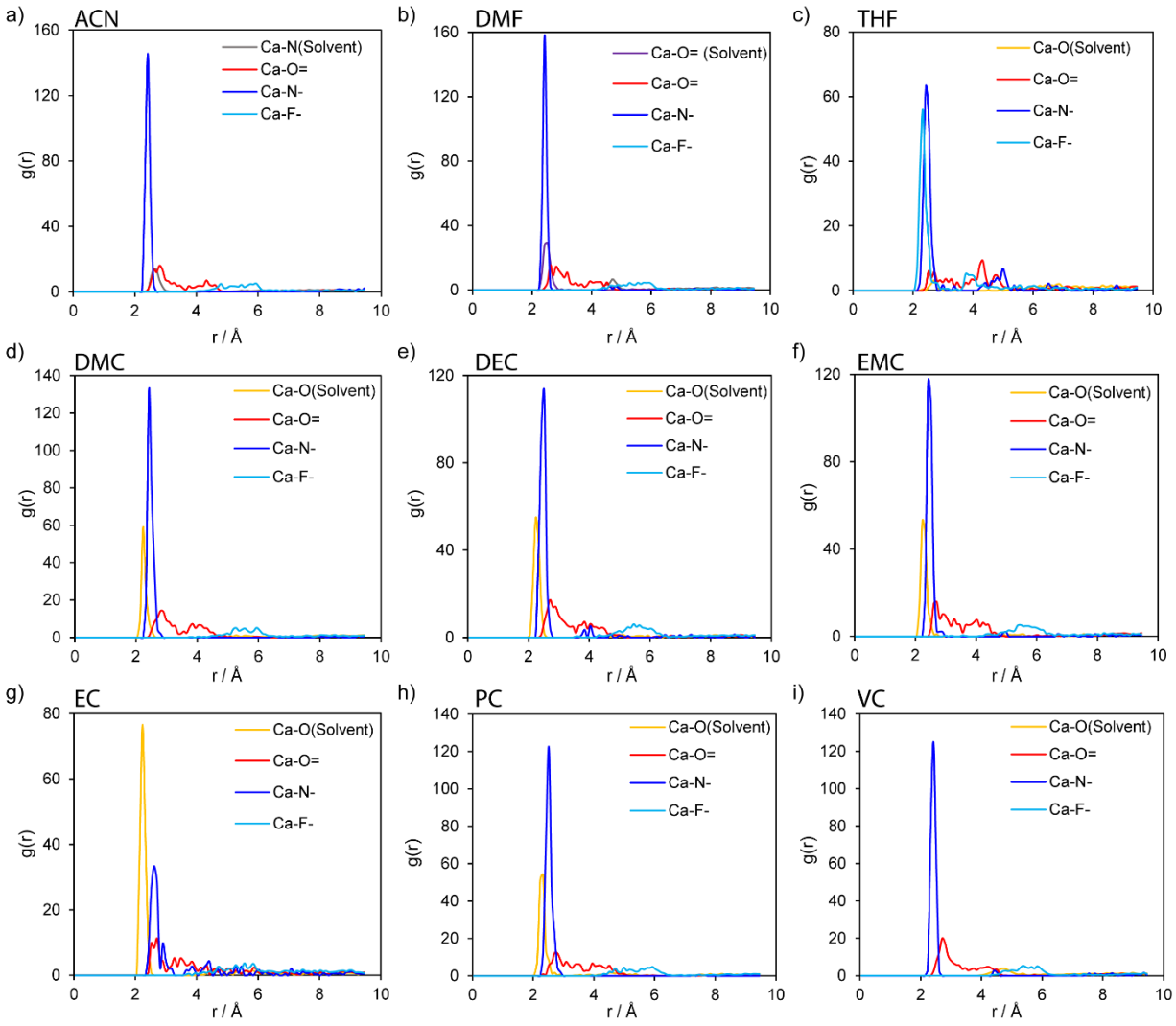

Figure 3. Radial distribution functions for electrolytes with single organic solvents and $Ca(TFSI)_2$. Solvents shown are (a-i) ACN, DMF, THF, DMC, DEC, EMC, EC, PC, VC, respectively. Legend entries are of the form Ca-X(bond), where X is the coordinating atom, "bond" is how the coordinating atom is bonded to its molecule (single "-" or double bond "="). When it was possible to distinguish, the label "Solvent" used for O (yellow) and N (gray for ACN) is used to indicate coordinating atoms from the solvent molecules. Legend entries for the same element without this label are associated to the salt anion, TFSI. The RDFs indicate that O from either the TFSI (red) or solvent (yellow) are the primary coordinating atoms in the first solvation shell, with THF also including F (light blue).

Finally, examining the binary organic mixtures (Figure 4), all first solvation layers are defined by coordination to C=O of the solvent molecules, primarily from the EC. Beyond this first solvation shell, the N of TFSI is present (second peak in the RDFs). The position of the first peak for EC-DEC, EC-DMC, EC-EMC, EC-PC and EC-VC are 2.23, 2.32, 2.23, 2.32, and 2.23 Å. The probabilities for the coordination with atoms from the salt anion and solvent are similar for all except VC. The solvation structure of the binary solvents can also be rationalized based on the properties of the individual components. Overall, the

solvation shells are defined exclusively by the solvent atoms (e.g., O oxygen primarily from C=O bond of the molecule) with no significant pairing with the TFSI, indicating good solubility of the salt. In the case of binary organic solvents with $Ca(ClO_4)_2$, the RDFs (Figure S7) also show that the first peak and greater probability is for the O from the C=O function of the EC molecule. However, the O from the perchlorate appears as the second major peak with a relatively significant probability, which contrasts with the results for the binary organic solvents with TFSI, in which coordination with TFSI is not observed. Hence, the RDFs indicate that the solvated structures show the binary organic mixtures can reduce pairing with the salt anion (both $TFSI^-$ and ClO_4^-), as the first peak in the RDFs is always associated to the O atoms of the solvent molecules.

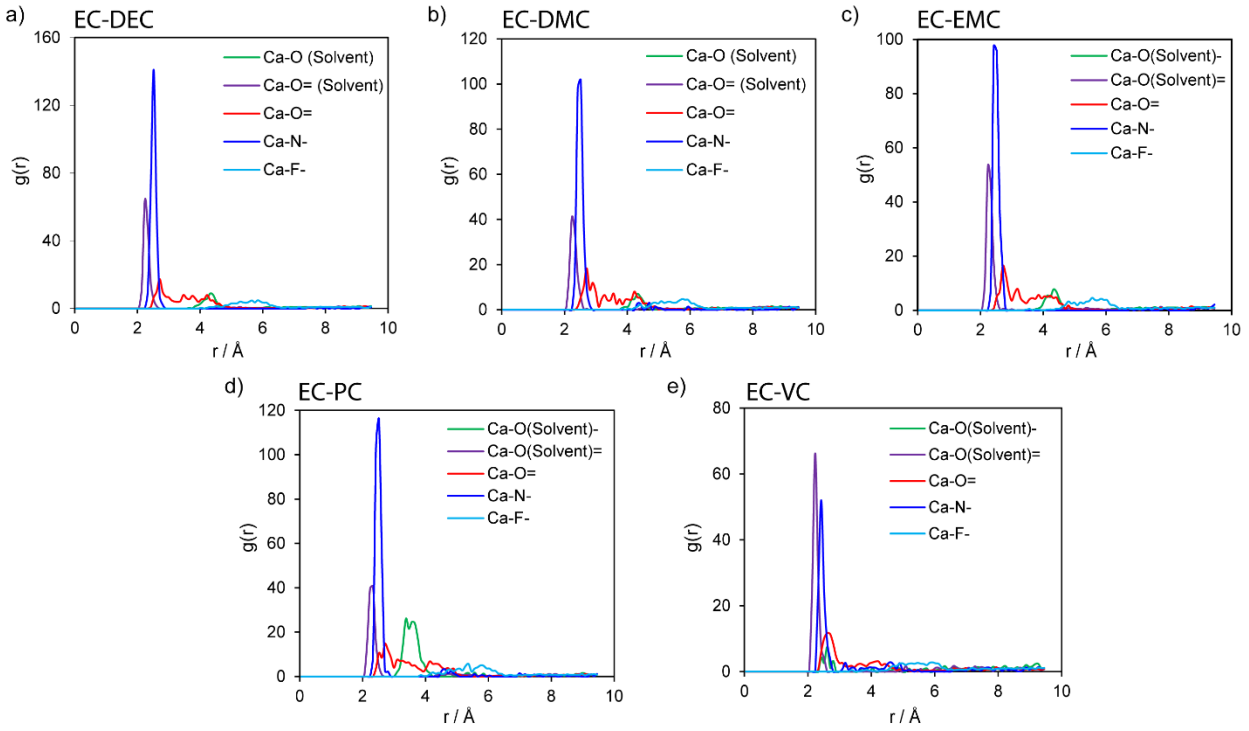

Figure 4. Radial distribution functions for electrolytes with binary organic solvents and $Ca(TFSI)_2$. Solvents shown are (a-e) EC-DEC, EC-DMC, EC-EMC, EC-PC, and EC-VC, respectively. Legend entries are of the form Ca-X(bond), where X is the coordinating atom, "bond" is how the coordinating atom is bonded to its molecule (single "-" or double bond "="). When it was possible to distinguish, the label "Solvent" used for O (green, purple) is used to indicate coordinating atoms from the solvent molecules. Legend entries for the same elements without this label are associated to the salt anion, TFSI. The RDFs indicate that O from the solvent, primarily the EC (purple) and the N from the TFSI are the primary coordinating atoms in the first solvation shell.

3.2. Coordination Structure

To further elucidate the structure of the coordination environment, we examined the Ca^{2+} solvated complexes. **Figures 5-7** show images of coordination environment for Ca^{2+} in the electrolytes as well as a tabulation of the coordinating atoms and their source molecules based on counting statistics. Beginning with discussion on the IL electrolytes (**Figure 5**), the solvated structure confirms the primary coordination atoms are O and N from either the IL anion, or salt anion, or both. The structures show the anions coordinate to Ca^{2+} bi- or tri-dentately. [EMIM][Otf], [BMP][TFSI], [EMIM][MESO3] and [BMIM][Otf] are primarily coordinated to Ca^{2+} via an O atom of the anion, [EMIM][TFSI] and [HMIM][Cl] via the N atom (from the TFSI anion), with [HMIM][Cl] also showing Cl^- coordination from the IL's anion. The large amount of coordination to N with [EMIM][TFSI] is commensurate with its RDF. That all solvated structures show N coordination confirms some degree of ion pairing with the TFSI is always present (be it from the salt or IL for [BMP][TFSI] and [EMIM][TFSI]). We could distinguish between the source of the O atoms from either the IL (solvent) or the TFSI anion (other), except for [BMP][TFSI] and [EMIM][TFSI] in which TFSI is the anion for both, but nevertheless, it shows that coordination among all IL systems to an O source is primarily with the TFSI anion. However, coordination to the IL anion (solvent oxygen) is present with [EMIM][Otf], [EMIM][MESO3], and [BMIM][Otf], and their anions all have in common the SO_3^- substructure. This may indicate preference for coordination with smaller anions, or ones with less steric hindrance, as would be found with TFSI. Indeed, we do observe that if the TFSI is the common anion for both the IL and salt ([BMP][TFSI], [EMIM][TFSI] and [HMIM][Cl]) or dominates over the IL anion (i.e., [HMIM][Cl]), then coordination with multiple atoms from a single TFSI (i.e., O and N) is present, which perhaps better stabilizes Ca^{2+}. Whereas, when the IL anion is different (i.e., [EMIM][Otf], and [EMIM][MESO3], and [BMIM][Otf]), there is more shared coordination with TFSI. The small degree of coordination of [EMIM][Otf] and [EMIM][MESO3] to the IL anion (sulfonate group) is commensurate with their respective RDFs.

With regards to observations when using $Ca(ClO_4)_2$ as the salt with IL solvents (Figure S8), the images reveal that there is greater coordination with the anion of the IL than the salt anion (ClO_4^-) as compared to electrolytes with $Ca(TFSI)_2$, with [HMIM][Cl] being the exception. The structures show the anions (from IL or salt) coordinate to Ca^{2+} mono-dentately. One other observation is that switching from a salt anion of $TFSI^-$ to ClO_4^- removes the possibility of coordinating to an N atom, which allows better coordination to the IL anion ([EMIM][Otf], [HMIM][Cl], [EMIM][MESO3], and [BMIM][Otf]). This is also indicated by [BMP][TFSI] and [EMIM][TFSI] which show increased coordination to N when the IL anion is TFSI ([BMP][TFSI] and [EMIM][TFSI]). This may allow us to conclude that the coordinating strength (and ion pairing) with the salt and/or more solvation by the IL can be achieved when no coordinating N atoms are present. The sulfonate anions of the ILs are also able to displace the ClO_4^- more so than the $TFSI^-$. These

differences manifest significantly in the solvation energetics, but not as much with Ca^{2+} mobility (See Sections 3.3 and 3.4).

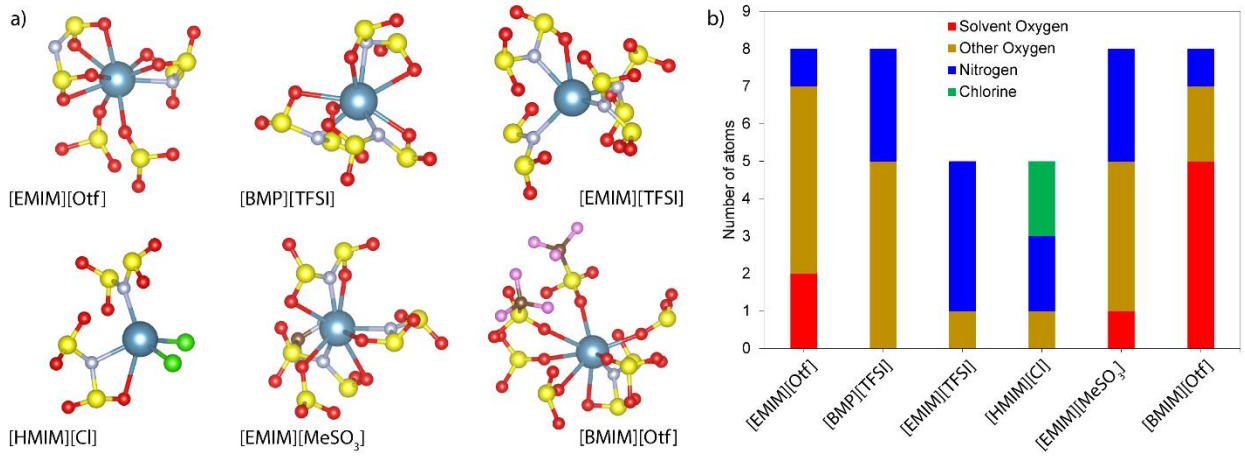

Figure 5. Examination of the solvation layer for the IL solvents with $Ca(TFSI)_2$. (a) Snapshots of the solvated Ca^{2+}-complexes for the six ionic liquids investigated. (b) Summary of the coordinating atoms classified by their associated molecule. Color code for atoms in a) are: Red is oxygen, sulfur is yellow, light blue is nitrogen, green is chlorine, fluorine is pink. Some atoms from the molecules are not represented owing to truncating zoom in to view the structures. Nitrogen comes from the salt anion $TFSI^-$. Oxygen and nitrogen sources are ambiguous for [BMP][TFSI] and [EMIM][TFSI], owing to same $TFSI^-$ anion as the salt ($Ca(TFSI)_2$). The data shows that the first solvation shell comprises of coordination to both the solvent and salt anion (i.e., ion-pairing).

Figure 6 shows solvation structures and a summary of the coordinating atoms for single organic solvents. The structures show the salt anions coordinate to Ca^{2+} bi-dentately. The first noticeable system is EC, in which the Ca^{2+} is fully solvated by 8 molecules. This may be compared to a $Ca(BF_4)_2$ system in which there is ion pairing with one BF_4^- anion.[28] DMC, DEC, and EMC partially solvate Ca^{2+} (5, 4, and 4 molecules, respectively) with the remainder of the solvation shell composed of the O or the N atom of the salt's $TFSI^-$ anion. DMF is comparable to DEC and EMC (in terms of solvent coordination), but one less $TFSI^-$ (salt anion) molecule (O) coordinating to it. PC follows with 3 coordinating O, and more N coordination from the salt than oxygen. VC entails the largest (10) number of coordinating molecules, with 7 O from the solvent, and the remainder with the O or N of the salt anion. VC is an example where the solvated structures show Ca^{2+} well-coordinated to solvent molecules, while its respective RDF indicates a greater probability of the solvation shell consisting of the salt anion. This difference is resolved by examining the running integral, n(r), of the RDF to count the respective number of coordinate atoms from the solvent and salt anion, which shows that indeed VC does coordinate to Ca^{2+} in greater number than the salt anion (See Supporting Information). THF provides only one O to the coordination shell, with one N from the salt anion and, interestingly, strong coordination to the F from the TFSI anion. This may be associated to the weaker

coordination strength of the ether oxygen, relative to that of the salt anion, as compared to coordination to the C=O as present with other carbonate electrolytes. ACN also shows strong coordination of its N with Ca^{2+}, which can be explained by its relatively smaller size and large electron density surrounding the N atom. Among these specific observations, a broader one is that ion pairing with the salt is generally present to varying degrees, with EC possibly being an exception. The tabulation of coordinating atoms in the solvation shell and their source molecule (Figure 6b) are commensurate with the radial distribution probabilities (Figure 2), namely whether it is the solvent or anion (or both) that defines and/o comprises the first solvation layer.

With regards to observations when using $Ca(ClO_4)_2$ as the salt with single organic solvents (Figure S9 Information), the structures show the salt anions coordinate to Ca^{2+} mono-dentately. Generally, more atoms are involved in the solvation of Ca^{2+}. This is generally manifested by more solvent molecules in the Ca^{2+} complexes, yet ion pairing with ClO_4 is present. Oxygen is the sole coordinating atom from either the solvent and ClO_4, except for the N of ACN. This contrasts with TFSI, which is present in greater numbers than ClO_4. This indicates that Ca^{2+} coordination with $TFSI^-$ is more likely that than with ClO_4, which can be explained by TFSI having multiple possible coordinating atoms (O, N, even F) as revealed in Figure 5b. Examples of coordination with N and o from the same TFSI anion can be found complexes such as with DMC, DEC, and EMC. These differences manifest significantly in the solvation energetics, and, unlike the ILs, noticeably with Ca^{2+} mobility (See Sections 3.3 and 3.4).

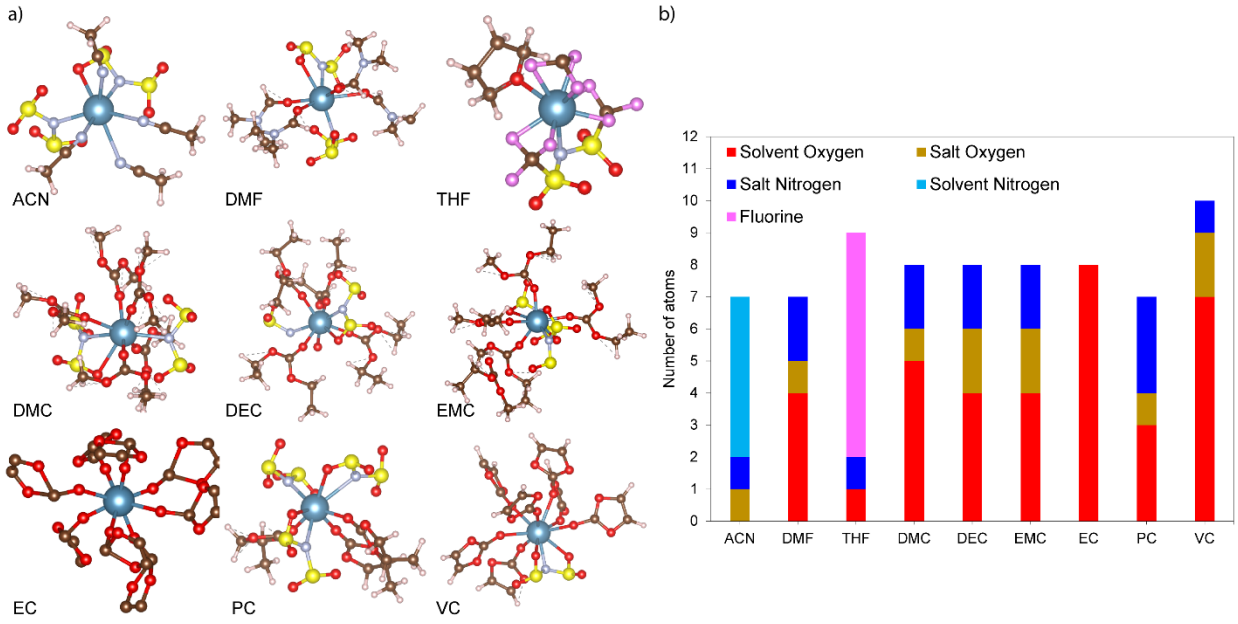

Figure 6. Examination of the first solvation layer for the single organic solvents with Ca(TFSI)2. (a) Snapshots of the Ca^{2+} complexes. (b) Summary of the coordinating atoms classified by the source. Color code for atoms in a) are:

Red is oxygen, sulfur is yellow, light blue is nitrogen, green is chlorine, fluorine is pink. Some atoms from the molecules are not represented owing to truncating zoom in to view the structures. Fluorine comes from the salt anion TFSI. The data shows that the first solvation shell comprises of coordination to both the solvent and salt anion (i.e., ion-pairing).

Figure 7 shows solvation structures and a summary of the coordinating atoms for binary organic solvents. The structures show the salt anions coordinate to Ca^{2+} mono- or bi-dentately. The addition of EC to DEC, DMC, and EMC increases the number of coordinating solvent molecules, which is understood by EC's stronger ability to coordinate with Ca^{2+} as revealed by the snapshots in Figure 6a. EC-PC has reduced solvent coordination, once again as expected based on the solvating capability of the individual molecules. EC-VC remains an outlier with its properties, which might indicate that VC allows for pairing with the salt anion, more so than EC can induce a fully solvated structure. This may be owing to the greater charge delocalization from VC diminishing the capability to solvate Ca^{2+}. The images for EC-PC and EC-VC and their tabulated atoms for the coordination environment show that PC and VC contribute no (or very few) oxygens to the solvation structure. It appears that PC and VC increase the propensity for ion pairing with TFSI, where pure EC alone mitigates this effect. Our solvated structures also are commensurate to experimentally determined solvent solvation numbers, particularly for EC (5) and DMF (6) determined elsewhere.[26] Notably binary mixtures of cyclic carbonates (i.e., EC-PC) always show coordination with the C=O of the respective molecules. Whereas, when the second carbonate (non-EC molecule) is acyclic, there was a mix of coordination to either the O of its carbonyl (C=O) or ether (C-O-C), perhaps owing to the greater flexibility of the molecule allow the possibility for stabilized structures to ensure with coordination to either group.

With regards to observations when using $Ca(ClO_4)_2$ with binary organic solvents (Figure S10), the structures show the salt anions coordinate to Ca^{2+} mono-dentately. Greater coordination with O from the solvent molecules is observed, as with the single organic solvents. There is a slightly greater number of coordinating atoms in the solvated structures, and greater contributions by the non-EC molecules. Noticeably, ion pairing with the salt anion is reduced when using $Ca(ClO_4)$, and is not present to a significant degree with EC-DMC and EC-PC. Once again, the reasons for these observations are like those described for single organic solvents, name the lack of coordinating N atoms. The differences between the second carbonate being cyclic or acyclic are similar to those with $Ca(TFSI)_2$, which PC being an exception. This may be related to the ease in displacement of the perchlorate anion balancing out differences between cyclic and acyclic carbonates. All such differences manifest significantly in the solvation energetics, only slightly with Ca^{2+} mobility (See Sections 3.3 and 3.4).

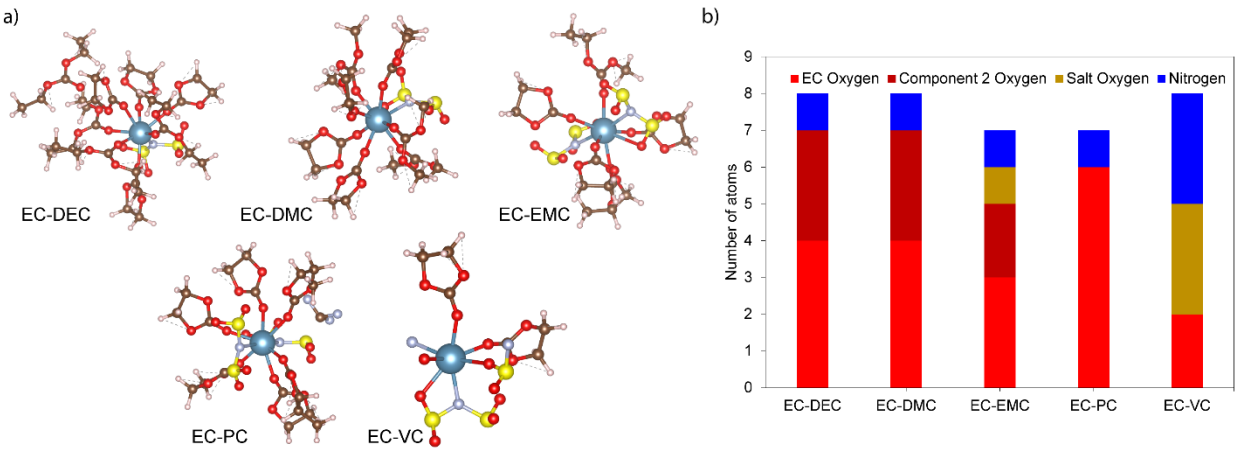

Figure 7. Examination of the first solvation layer for the binary organic solvents with Ca(TFSI)2. (a) Snapshots of the Ca^{2+} complexes. (b) Summary of the coordinating atoms classified by the source. Color code for atoms in a) are: Red is oxygen, sulfur is yellow, light blue is nitrogen, and green is chlorine. Some atoms from the molecules are not represented owing to truncating zoom in to view structures (such as F). Nitrogen comes from the salt anion TFSI. The data shows that the first solvation shell comprises of coordination mostly to the solvent and to a lesser extent the salt anion (i.e., ion-pairing).

To assess the quantity of solvent molecules solvating Ca^{2+} more rigorously, Figure 8 provides a summary of the solvation numbers (SN) both for solvent and salt anion molecules, determined from the running integral, n(r), of the radial distribution functions (Figures S11-S16). Plots of the running integrals are provided in Figures S9-S14. Several key findings are revealed in the summary of coordinating atoms and molecules. For ionic liquids, significant pairing to the salt anion is observed with $Ca(TFSI)_2$, whereas the presence of the IL and salt anion in the solvation structure is more balanced with $Ca(ClO_4)_2$. Mixed coordination (N and O) is present for $Ca(TFSI)_2$, and O is the primary coordinating atom for $Ca(ClO_4)_2$. For single organic solvents, the first solvation shell is dominated by O from the solvent with $Ca(TFSI)_2$, but more balance for $Ca(ClO_4)_2$ (yet with solvent O still in greater number). These points are the same for ACN, but apply to its N atom. For binary organic mixtures, the solvation structure primarily contains coordination to the O from the solvent, and to a lesser extent coordination to the salt anion. Lack of the second solvent component (other than EC) in the summary of the coordination structure is an artifact of the 2.8 Å cut-off set by the bond distance between Ca^{2+} and the O from the carbonyl group. Figure 7 shows examples where coordination to the other solvent molecule is indeed present (e.g., DEC, DMC, EMC, PC). Similarly, while VC does not show in the summary of coordinating molecules in Figure 7, which is based on statistical counting of only atoms with direct bonds to Ca^{2+}, based on the n(r) data (Figure 8) VC is included in the solvation structure. Importantly, the number of solvent molecules present in the first solvation shell are comparable to the experimentally determined solvent solvation numbers ($SN_{solvent}$) for DMF (6), EC (5),

and PC (4).[26] In the case of DMF, for example, the average number of coordination solvent was experimentally measured to be 7.2 and theoretically determined to be stable at 8.[29, 45] Consideration of ion pair with the TFSI and ClO_4 places the values determined herein to be less, yet with the same approximate total number of coordinating molecules of ~7-8.

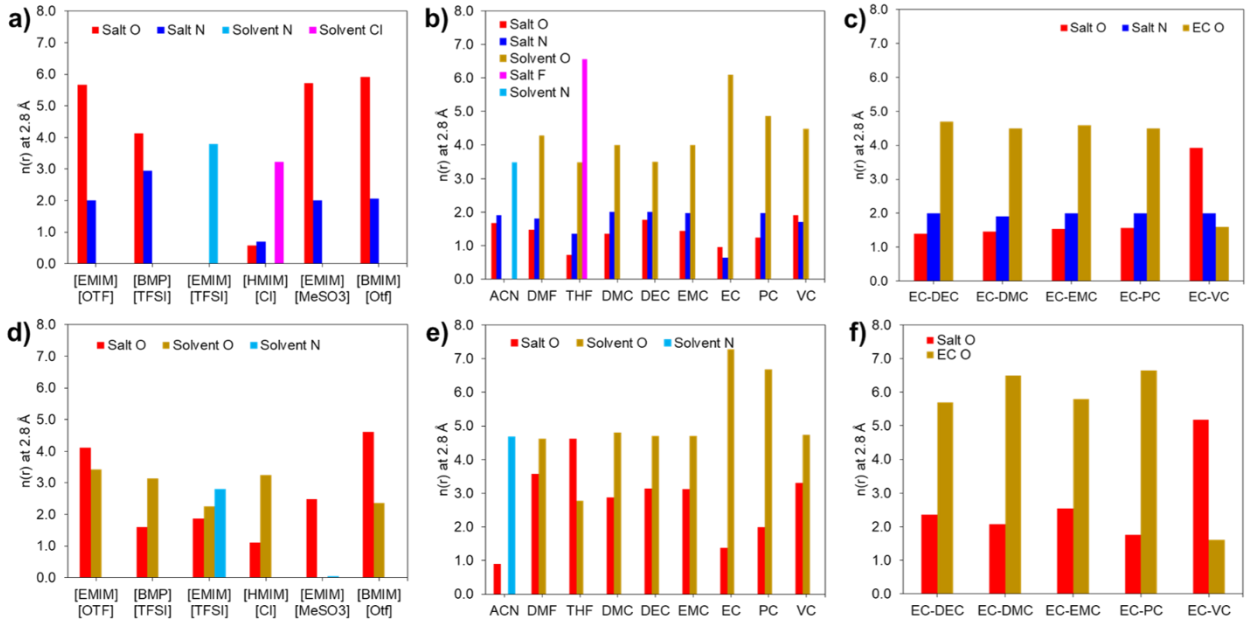

Figure 8. Solvation numbers for both solvent and salt anions determined from the n(r) values at a 2.8 Å radial distance from Ca^{2+} centers for (a) $Ca(TFSI)_2$ and (b) $Ca(ClO_4)_2$. Solvating molecules (solvent and salt) are identified by their coordinating atom. The cut-off of 2.8 Å is selected owing to this being the Ca^{2+}-O bond distance. More balanced coordination between the solvent and salt anion is observed for ClO_4 over TFSI. Organic solvent molecules (single and binary) show a larger present in the first solvation shell as compared to ionic liquids.

3.3. Solvation Energetics

Figure 9 shows calculated solvation energies of all electrolytes explored. Several notable observations and conclusions can be made. Firstly, the solvation energies are smaller in magnitude for $Ca(ClO_4)_2$ than for $Ca(TFSI)_2$ for all solvents, and furthermore, all solvation energies are smaller in magnitude than those, respectively, calculated with $Ca(BF_4)_2$ as the salt ($|\Delta G|$ values of 411.77, 384.59, 397.93, 446.11, 463.05, 459.99, 397.30, 402.84, 462.77, and 472.18 kcal/mol for EC, VC, PC, DMC, EMC, DEC, EC-PC, EC-DMC, EC-DMC and EC-DEC, respectively),[28] while we reserve definitive conclusion on this latter point owing to possible differences in the calculation methods between the implicit model used herein and the explicit model employed by other's work. Calculated energies are similar to those calculated for DMF.[29] Nevertheless, indeed, the general trend for the absolute value $|\Delta G|$ with respect to salt, $Ca(ClO_4)_2$ < $Ca(TFSI)_2$ < $Ca(BF_4)_2$, which overall may be associated to the reduced ion pairing and better solvation by

the solvents, and is also consistent with the ease of ion–ion dissociation from the TFSI and ClO_4 anions enabling relatively good solubility, as observed experimentally.[26] For both salts, the smallest solvation energies are found for DEC, DMC, and EMC, followed closely by THF. Above these energies, all IL, single organic, and binary organic solvation energies are greater than ~150 kcal/mol in magnitude. The differences in the solvation structures for the ionic liquids do not appear to make a significant difference in the solvation energies for their respective solvent class (IL, single organic, binary organic), nor are there significant differences for solvation structures dominated by O or N atoms, showing that both are sufficient to reach similar thermodynamically stable solvated structures. Increases in $|\Delta G|$ are observed when transitioning from single to binary organic solvents. DMF, EC, and PC, and to some extent THF appear to be exceptions, providing similar $|\Delta G| > 200$ kcal/mol, and THF an intermediate value between those of the single and binary solvents.

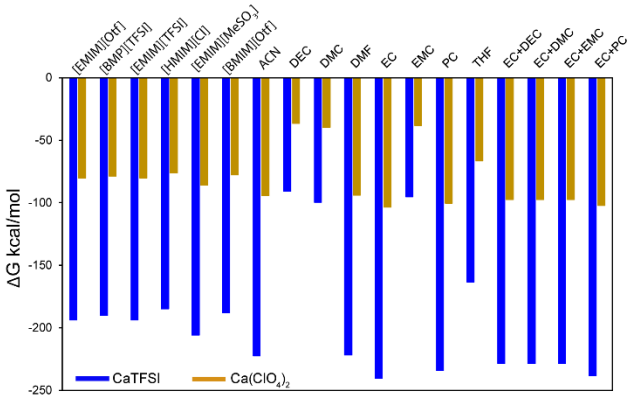

Figure 9. Summary of the free energy of solvation of Ca^{2+}-complexes for all solvent-salt systems at 298 °K. VC electrolytes not included owing to lack of a suitable dielectric constant. With $Ca(ClO_4)_2$ complexes with lower solvation energies are produced, as compared to $Ca(TFSI)_2$. The lowest solvation energies (for both salts) are produced for DEC, DMC, EMC, and THF.

Generally, greater solvation energies are interpreted to imply well-solvated structures; however, this conclusion must include (and be confirmed by) the examination of the structure and composition of the solvation layer (i.e., source molecules from either the solvent or salt anion), because ion pairing with the salt anion (which is undesirable) can also increase the magnitude of the solvation energy. Previous calculations of ΔG showed a noticeable increase in ΔG between solvation shells that contain 1 and 2 salt anions,[28] which implies that ion pairing contributes more so to greater $|\Delta G|$. Herein, increase in solvation energy, for example when comparing single organic solvents to binary ones, is accompanied by an increase of Ca^{2+} solvation by solvent molecules (i.e., less pairing with the salt anion). In short, greater solvation energy comes from greater solvent coordination to Ca^{2+}. Likewise, switching from $TFSI^-$ to ClO_4^- also yields better solvation. Hence, it can be concluded that indeed there is good solvation for both $Ca(TFSI)_2$

and $Ca(ClO_4)_2$ in binary solvents, as they show both well solvated structures as greater |ΔG|. Yet, some solvents showed both smaller values for ΔG and also well-solvated Ca^{2+}, and this combination can further imply higher mobility and electrochemical kinetics (i.e., via more facile solvation and desolvation).[46-48] For example, both ACN and EC show that Ca^{2+} is well solvated by the solvent molecules, and combined with lower solvation energies would indicate good electrolyte systems from both a solvation and mobility standpoint, which can explain why both are effective in electrochemical studies.[11, 35] This is furthermore the case with electrolytes that use $Ca(ClO_4)_2$: they show combined observations of greater solvent solvation and smaller solvation energies, which implies both good solubility as well as mobility. Specifically, the ΔG values for all electrolytes with $Ca(ClO_4)_2$ and solvents DEC, DMC, EMC with $Ca(TFSI)_2$ are comparable to those calculated for $LiPF_6$, $NaClO_4$, and $Mg(ClO_4)_2$,[28] which may promise to provide comparable electrolyte mobilities as other incumbent electrolytes for other ion systems. Combining the observation of increase solvation of Ca^{2+} by the solvent molecules for binary organic mixtures when using $Ca(ClO_4)_2$, at its relatively lower solvation energies, would also indicate that both good solubility and now greater mobility can be expected.

3.4. Ca^{2+} Self-Diffusivity

Figure 10 shows Arrhenius plots of the calculated diffusivity of Ca^{2+} as a function of temperature for all solvent-salt electrolytes systems explored in this study. The diffusion coefficients specifically at 298.15 K are summarized in Figure 11. The first broad observation is that there are electrolytes from all solvent classes that yield comparable diffusivities, within the range of 10^{-6} to 10^{-5} cm^2/s. For the ionic liquids, the highest diffusivities are observed with [EMIM][Otf], [EMIM][MESO3], and [BMIM][Otf], for both $Ca(TFSI)_2$ and also $Ca(ClO_4)_2$, with the lowest diffusivities given by [HMIM][Cl], [EMIM][TFSI], and [BMP][TFSI] (the latter being the lowest). Among the electrolytes using a single organic solvent, there is a narrower range of diffusivities for $Ca(TFSI)_2$ salt, and higher floor to their values. ACN and THF yield the highest (for both salts), and EC and PC the lowest. Binary solvents are also in relatively the same range among themselves, and slightly higher in the range for $Ca(TFSI)_2$ over $Ca(ClO_4)_2$. Top diffusivities are provided by EC-DMC (for both salts), followed closely and together by EC-PC, EC-DEC, and EC-EMC. VC and EC-VC appear to be anomalies, with the former showing good diffusivity, but the latter showing a low one. Examples with diffusivities being higher with one salt over the other, and vice versa, are also observed. Explanations for all these differences is quite complicated, but certainly depend on the molecule size, structure, charge, etc. That they span only one order of magnitude range (10^{-6} to 10^{-5}), might make such differences insignificant in experimental studies. Nevertheless, towards selecting electrolytes with the highest diffusivity, electrolytes that would show good transport and solvation properties are: (ILs) [EMIM][Otf], [EMIM][MESO3], and [BMIM][Otf], (single organics) ACN and EMC, and (binary

organics) EC-DMC, EC-DEC, and EC-EMC (with EC-PC being competitive as well). Yet, other solvents with lower diffusivities are remain viable candidates. The higher diffusivities of $Ca(TFSI)_2$ electrolytes is commensurate with experimental investigations of ion conductivity in $Ca(TFSI)_2$ electrolytes with EC-PC as the solvent.[12, 26]

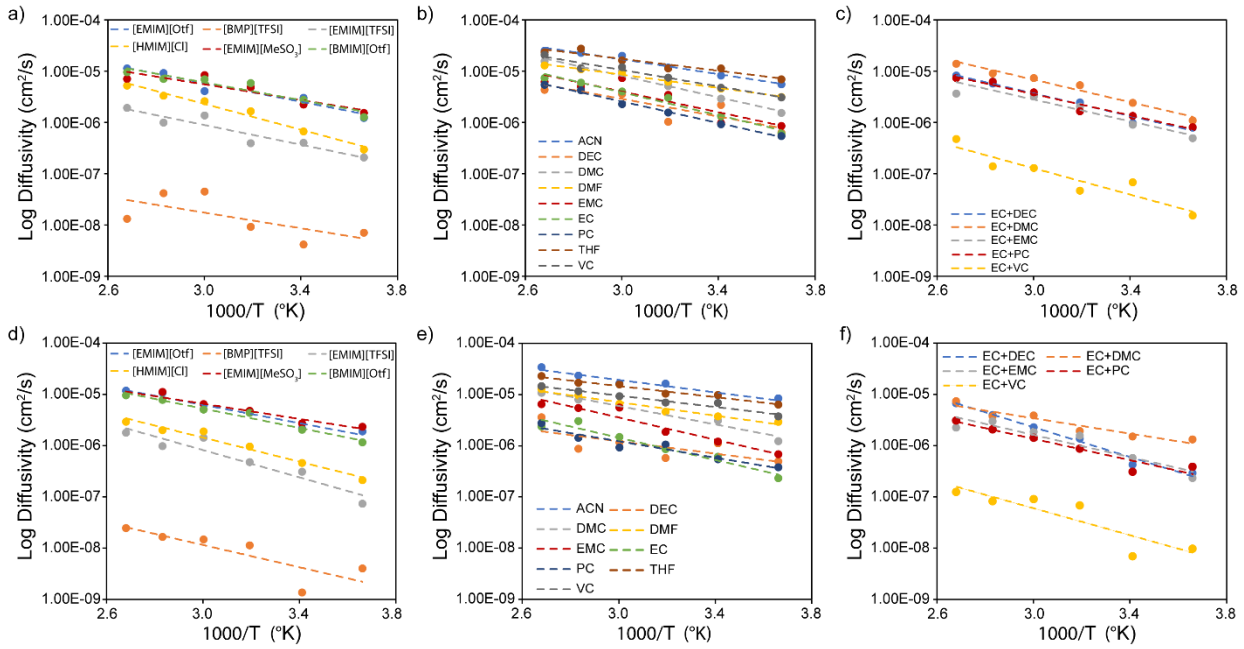

Figure 10. Theoretical Arrhenius plots of Ca^{2+} diffusivity as a function of temperature for solvents with (a-c) $Ca(TFSI)_2$ and (d-f) for $Ca(ClO_4)_2$, for ionic liquid, single organic, and binary organic solvents from left to right, respectively.

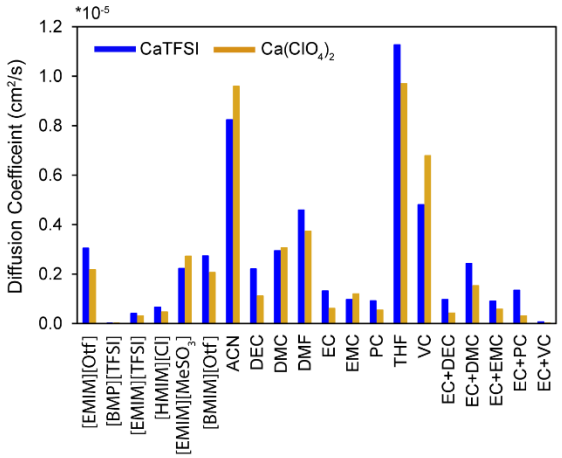

Figure 11. Diffusivity for electrolytes composed of the ionic liquid, organic, and binary organic solvents at T = 298 °K. Notably high diffusion coefficients are found for AC, DMF, THF, and DMC.

Establishing correlations between the diffusivity and the correspond solvated structures and energetics is complicated. It appears that all the marked differences in solvation structure energetics in turn yield mild differences in the Ca^{2+} mobility, at least for most of the systems. Yet some observations can be made. Indeed, reduced pairing with the salt anion correlates to greater diffusivities, as expected owing to salt-solvent coordination playing a key role in governing cation mobility in the electrolyte.[30] The order rank of diffusivity does follow closely the dielectric constants of the solvents (Table S1), as also affirmed in the literature.[26] ILs with only a sulfonate group would be preferable over TFSI for use as the solvent in electrolytes, as revealed by the relatively low diffusivity for [BMP][TFSI] and [EMIM][TFSI]. Reduced anion pairing is also achieved using acyclic molecules rather than cyclic ones, and $Ca(ClO_4)_2$ over $Ca(TFSI)_2$ in some cases, for both the single and binary organic solvents. Yet, the larger Ca^{2+} complexes (i.e., more molecules) when $Ca(ClO_4)_2$ is used may hinder mobility. Generalized understanding may be that (1) greater diffusivity is achieved via mixed coordination, provided from the TFSI anion (both O and N), rather than coordination solely an O atom, from the ClO_4 anion, (2) Ca^{2+} complexed presenting good solvation by the solvent molecules, but with less total coordinated molecules, (3) smaller solvent molecules (e.g., DMF, as well as DMC vs. DEC and EC-DMC vs EC-DEC), and (4) use of acyclic molecules (e.g., carbonates) with EC, (5) using of ILs with alkyl sulfonates as the anion. Note that another salt calcium trifluoromethanesulfonate ($Ca(TFS)_2$) shows comparable conductivities $Ca(TFSI)_2$ and $Ca(BF_4)_2$,[26] hence, the benefits of alkyl sulfonates may be further realized if $Ca(TFS)_2$ salt is explored in electrochemical studies. A focused study on different anions that specifically contain sulfonate groups would help reveal such similarities or differences and is the subject of future study. RT diffusivity values in which ClO_4 outdoes TFSI, such as ACN, VC, and [EMIM][MESO3], are exceptions with their own specific reasons (i.e., nitrile-based solvent, poor coordination, etc.). The proximity of diffusivity values for binary organic solvents shows that the better solvation properties with binary mixtures outdoes any enhancements by changing the salt, and this can allow for variation of electrolyte salt composition to optimize other electrolyte processes (e.g., redox reactions), SEI layer, anion intercalation, etc. That EC+VC shows a significantly lower diffusivity, combined with the lack of its involvement in the solvated structure, might indicate that its presence only impedes Ca^{2+} mobility.

3.5. Ionic liquid Stability at a Ca metal interface

While the decomposition of organic molecules such as carbonates has been examined for the resultant products, similar insight into ionic liquids is lacking. Owing to the results showing that some ILs can have favorable solvation properties, we finally investigated AIMD simulations specifically of [EMIM][Otf] interaction at a calcium metal interface. TFSI decomposition has already been investigated elsewhere,[49] leaving such alkyl sulfonates as with [EMIM][Otf] (and similarly [EMIM][MESO3] and [BMIM][Otf])

warranting inquiry. Figure 12 shows AIMD snapshots over a duration to 5000 fs in 1000 fs intervals. A simulation run time of 5000 fs was sufficient, as revealed by the stabilization of the system potential energy (Figure S17). The resulting coordinated structures reveal that both the anion and cation of the solvent molecule interact with the surface calcium atoms, but to different extents, and without completely breaking down to form any noticeable organic or inorganic decomposition products that would be expected to comprise the SEI layer. After 200 fs, the solvent cation appears to coordinate with the surface Ca atoms, whereas bonding of the solvent anion proceeds progressively, starting at 400 fs, when one oxygen atom of the $CF_3SO_3^-$ anion appears to bond with surface calcium atoms, followed by bonding of a second oxygen atom of the same anion, and lastly, bonding of all 3 oxygen atoms of the triflate anion molecule after 1000 fs. This progressive bonding may be attributed to the downward steric movement of the triflate anion which leads to close contact between the calcium metal surface and the atoms of the anion molecule. On the other hand, the solvent cation continues to interact with the surface calcium atoms over the course of the trajectory, but no bond-cleavage occurs, possibly owing to a combination of two factors: 1) lack of sufficient electrons from the calcium metal owing to the strength of the C–N bond (of the IL cation) and 2) the planar orientation of the molecule that causes highly uniform charge distribution on the solvent molecule itself, thereby preventing bond breakage. The effect of solvent molecule orientation on the breakdown dynamics is currently being explored and will be reported as a separate study. Nevertheless, it appears from these AIMD trajectories that the IL solvent molecules do not breakdown into any specific decomposition products. As for the time-scale of this simulation, we anticipate no further breakdown to occur beyond 1000 fs owing to the potential energy of the system having attained quasi-equilibrium at 1000 fs (see Supporting Information). Furthermore, 1000 fs is sufficient for all reaction dynamics to occur at the surface, as has been shown previously for ethylene carbonate on calcium metal.[31] As the imidazole subunit of [EMIM][Otf] is common among all ILs except [BMP][TFSI] (pyrrolidinium based), despite having varied alkyl lengths, it can be inferred that all such IL systems can be stable. However, Cl^- should generally be avoided owing to its tendency to cause corrosive effects on electrodes. Pyrrolidinium also might not necessarily break down, except perhaps through minimal hydrogen abstraction induced at the Ca surface. Given that [BMP][TFSI] and [EMIM][TFSI] contain $TFSI^-$ as the anion, which can break down, it may be concluded that [EMIM][Otf], [HMIM][Cl], [EMIM][MESO3], and [BMIM][Otf] (alkyl imidazole alkyl sulfonates) are stable against a Calcium interface, yet this is a subject of continued study. The lack of reductively stable electrolytes for Ca-metal batteries continues to be a major bottleneck in the Ca-battery field, and our preliminary results indicate the high stability of the [EMIM][Otf] solvent over Ca metal, which is a desirable characteristic from the standpoint of developing Ca metal anodes. [EMIM][Otf] has already shown effective for us in plating and stripping of Ca.[17] As such, further studies should focus on investigating Ca^{2+} transport

across these solvent-metal interfaces to possibly elucidate the ease of reversible deposition and dissolution of Calcium from bulk electrolyte.

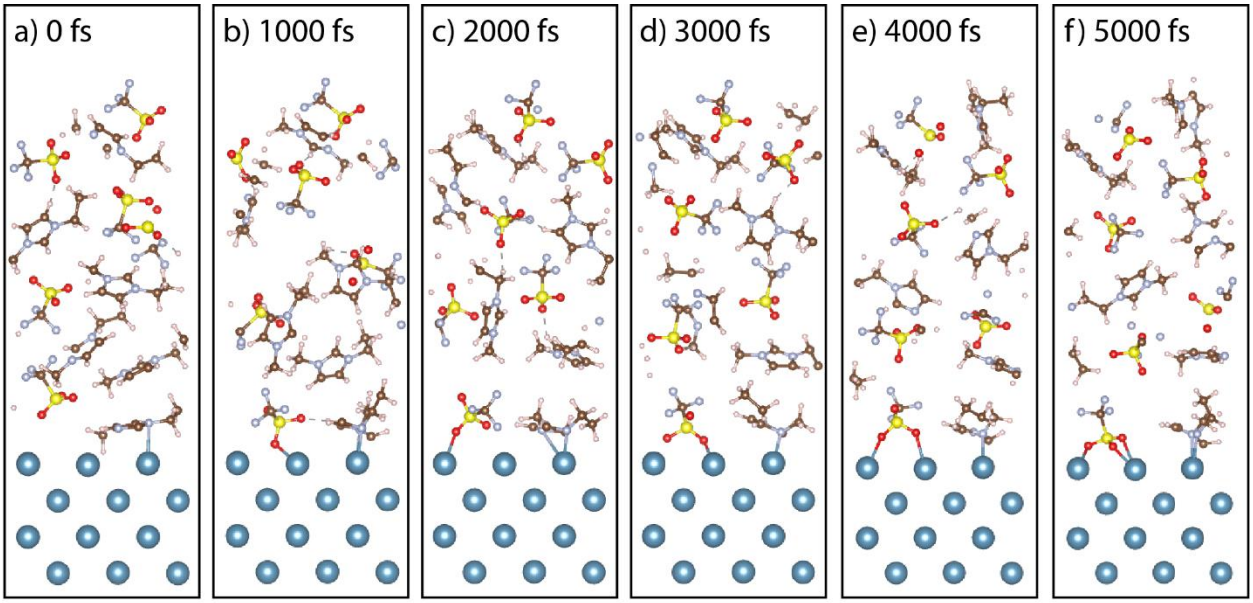

Figure 12. AIMD time-lapse snapshots of [EMIM][Otf] undergoing coordination over a Ca metal surface over the course of 5000 fs, in (a-f) snapshots in 1000 fs increments. Color code: Brown is carbon, light blue is nitrogen, yellow is sulfur, red is oxygen, white is hydrogen, pink is fluorine, and dark blue is calcium. [EMIM][Otf] does not undergo reductive decomposition, but rather coordinates with the Ca metal surface via the N from EMIM and O from Otf.

4. Key Aspects for Solvent Selection

Our results shows that several ILs have favorable electrolyte properties, specific those which do not contain a TFSI anion. The use of [EMIM][Otf] to achieve stable, reversible redox activity is also commensurate with its favorable electrolyte properties revealed herein, and similarly structure ILs (specifically with regards to the anion) may also be explored. There are a range of single organic electrolytes that can be used; and several have not yet been explored alone in eliciting redox activity at a Ca metal interface, such as DMF, among others. A range of binary organic solvents are also promising and may be explored in the context of enabling and advancing redox activity. Our results would indicate that use of a TFSI salt is preferable both with regards to solubility as well as mobility, and favorable electrolyte properties of the ionic liquids with alkyl sulfonates as the anion could also indicate that calcium trifluoromethanesulfonate ($Ca(TFS)_2$) may be a suitable salt to explore. $Ca(ClO_4)_2$ was previously attempted, and showed some very low levels of plating/stripping kinetics,[12] which may be associated to passivation by the decomposition products of the perchlorate, as observed in Li systems. This might be mitigated through the use of pre-passivation layers,[23, 25] to decouple the conductivity of $Ca(ClO_4)_2$ from the decomposition to form the solid

electrolyte interface, yet such experimental studies remain to be pursued. Likewise, TFSI has been previously used, but is preferable as the electrolyte in which a pre-passivated layer using another salt has been performed, as the decomposition products of TFSI appear unfavorable for Ca^{2+} transport across the SEI. Other than EC-PC, binary organic electrolytes remain to be thoroughly explored to correlate their electrolyte properties to Ca redox activity. Overall, differences among the electrolytes may become more apparent with regards to solvation and desolvation during redox reactions. Identified favorable electrolytes herein such as ACN, THF and EC+PC with $Ca(TFSI)_2$ show good diffusivities and are notably used in current battery studies,[35-37, 50-51] as well as THF and EC+PC, and even EC+EMC+DMC to enable redox activity at a calcium metal interface.[11-12, 14, 23, 25] Single solvents such as DMF, DEC, DMC, and EMC should also show good solubility and mobility, combined with possibly good desolvation to enable redox activity. Such experimental uses corroborate the theoretically acquired, generalized understanding herein, and reveal other electrolytes that may also be explored.

5. CONCLUSION

We have presented a study on the solvation structure, energetics, and diffusivity of Ca^{2+} in electrolytes cross-cutting several types of solvents, namely ionic liquids, carbonates, ethers, nitriles, and binary organic carbonate mixtures with $Ca(TFSI)_2$ and $Ca(ClO_4)_2$ as the two salts examined The results reveal several promising electrolyte systems in terms of reduced pairing with the salt anion, good solubility, and favorable Ca^{2+} mobility. The combination of well solvated Ca^{2+} complexes with the solvents as well as low free energies point towards the possibility of high concentration and highly conductive electrolytes. The results show that non-N containing ionic liquids (the anion), acyclic carbonates, DMF, THF, as well as several binary organic (EC-DMC, EC-EMC, EC-DEC) are all potentially favorable electrolytes. Using $Ca(TFSI)_2$ is preferred over $Ca(ClO_4)_2$ owing to better solvation and mobility, and possibly the salt Ca(TFS), but further experimental studies are required. This work provides theoretical insight that has revealed potential candidate electrolytes to be considered in electrochemical and cycling studies for calcium (ion) batteries.

ACKNOWLEDGEMENTS

The authors gratefully acknowledge funding supported The Syracuse Center of Excellence, the National Science Foundation under grant number CMMI-1751621, as well as support from the College of Engineering and Computer Science at Syracuse University.

SUPPORTING INFORMATION

- Summary of systems sizes used in LAMMPS and VASP simulations, and solvent dielectric constants
- Corresponding data for all solvents, specifically, RDF and solvated structures with $Ca(ClO_4)_2$
- Running integrals, n(r), for all electrolytes
- System potential energy for AIMD simulations

REFERENCES

1. Hosein, I. D., The Promise of Calcium Batteries: Open Perspectives and Fair Comparisons. *ACS Energy Lett.* **2021**, *6*, 1560-1565.
2. Stievano, L.; de Meatza, I.; Bitenc, J.; Cavallo, C.; Brutti, S.; Navarra, M. A., Emerging Calcium Batteries. *J. Power Sources* **2021**, *482*, 228875.
3. Nielson, K. V.; Liu, T. L., Dawn of Calcium Batteries. *Angewandte Chemie International Edition* **2020**, *59*, 3368-3370.
4. Gummow, R. J.; Vamvounis, G.; Kannan, M. B.; He, Y. H., Calcium-Ion Batteries: Current State-of-the-Art and Future Perspectives. *Adv. Mater.* **2018**, *30*, 1801702.
5. Arroyo-de Dompablo, M. E.; Ponrouch, A.; Johansson, P.; Palacín, M. R., Achievements, Challenges, and Prospects of Calcium Batteries. *Chem. Rev.* **2019**, *120*, 6331–6357.
6. Ponrouch, A.; Palacin, M. R., On the Road toward Calcium-Based Batteries. *Curr. Opin. Electrochem.* **2018**, *9*, 1-7.
7. Monti, D.; Ponrouch, A.; Araujo, R. B.; Barde, F.; Johansson, P.; Palacín, M. R., Multivalent Batteries—Prospects for High Energy Density: Ca Batteries. *Front Chem* **2019**, *7*, 1-6.
8. Muldoon, J.; Bucur, C. B.; Gregory, T., Quest for Nonaqueous Multivalent Secondary Batteries: Magnesium and Beyond. *Chem. Rev.* **2014**, *114*, 11683-11720.
9. Melemed, A. M.; Khurram, A.; Gallant, B. M., Current Understanding of Nonaqueous Electrolytes for Calcium-Based Batteries. *Batteries & Supercaps* **2020**, *3*, 570-580.
10. Liang, Y.; Dong, H.; Aurbach, D.; Yao, Y., Current Status and Future Directions of Multivalent Metal-Ion Batteries. *Nature Energy* **2020**, *5*, 646-656.
11. Biria, S.; Pathreeker, S.; Li, H.; Hosein, I. D., Plating and Stripping of Calcium in an Alkyl Carbonate Electrolyte at Room Temperature. *ACS Appl. Energy Mater.* **2019**, *2*, 7738-7743.
12. Ponrouch, A.; Frontera, C.; Barde, F.; Palacin, M. R., Towards a Calcium-Based Rechargeable Battery. *Nat. Mater.* **2016**, *15*, 169-173.
13. Biria, S.; Pathreeker, S.; Genier, F. S.; Chen, F.-H.; Li, H.; Burdin, C. V.; Hosein, I. D., Gel Polymer Electrolytes Based on Cross-Linked Poly(Ethylene Glycol) Diacrylate for Calcium-Ion Conduction. *ACS Omega* **2021**, *6*, 17095-17102.
14. Wang, D.; Gao, X. W.; Chen, Y. H.; Jin, L. Y.; Kuss, C.; Bruce, P. G., Plating and Stripping Calcium in an Organic Electrolyte. *Nat. Mater.* **2018**, *17*, 16-20.
15. Li, Z.; Fuhr, O.; Fichtner, M.; Zhao-Karger, Z., Towards Stable and Efficient Electrolytes for Room-Temperature Rechargeable Calcium Batteries. *Energy Environ. Sci.* **2019**, *12*, 3496-3501.
16. Shyamsunder, A.; Blanc, L. E.; Assoud, A.; Nazar, L. F., Reversible Calcium Plating and Stripping at Room Temperature Using a Borate Salt. *ACS Energy Lett.* **2019**, *4*, 2271-2276.
17. Biria, S.; Pathreeker, S.; Genier, F. S.; Li, H.; Hosein, I. D., Plating and Stripping Calcium at Room Temperature in an Ionic Liquid Electrolyte. *ACS Appl. Energy Mater.* **2020**, *3*, 2310–2314.
18. Gao, X.; Liu, X.; Mariani, A.; Elia, G. A.; Lechner, M.; Streb, C.; Passerini, S., Alkoxy-Functionalized Ionic Liquid Electrolytes: Understanding Ionic Coordination of Calcium Ion Speciation for the Rational Design of Calcium Electrolytes. *Energy Environ. Sci.* **2020**, *13*, 2559-2569.

19. Stettner, T.; Dugas, R.; Ponrouch, A.; Balducci, A., Ionic Liquid-Based Electrolytes for Calcium-Based Energy Storage Systems. *J. Electrochem. Soc.* **2020**, *167*, 100544.
20. Nielson, K. V.; Luo, J.; Liu, T. L., Optimizing Calcium Electrolytes by Solvent Manipulation for Calcium Batteries. *Batteries & Supercaps* **2020**, *3*, 766-772.
21. Hahn, N. T.; Driscoll, D. M.; Yu, Z.; Sterbinsky, G. E.; Cheng, L.; Balasubramanian, M.; Zavadil, K. R., Influence of Ether Solvent and Anion Coordination on Electrochemical Behavior in Calcium Battery Electrolytes. *ACS Appl. Energy Mater.* **2020**, *3*, 8437-8447.
22. Wang, M.; Jiang, C. L.; Zhang, S. Q.; Song, X. H.; Tang, Y. B.; Cheng, H. M., Reversible Calcium Alloying Enables a Practical Room-Temperature Rechargeable Calcium-Ion Battery with a High Discharge Voltage. *Nat. Chem.* **2018**, *10*, 667-672.
23. Forero-Saboya, J.; Davoisne, C.; Dedryvère, R.; Yousef, I.; Canepa, P.; Ponrouch, A., Understanding the Nature of the Passivation Layer Enabling Reversible Calcium Plating. *Energy Environ. Sci.* **2020**, *13*, 3423-3431.
24. Jie, Y. L., et al., Electrolyte Solvation Manipulation Enables Unprecedented Room-Temperature Calcium-Metal Batteries. *Angew. Chem. Int. Edit.* **2020**, *59*, 12689-12693.
25. Song, H.; Su, J.; Wang, C., Hybrid Solid Electrolyte Interphases Enabled Ultralong Life Ca-Metal Batteries Working at Room Temperature. *Adv. Mater.* **2021**, *33*, 2006141.
26. Forero-Saboya, J. D.; Marchante, E.; Araujo, R. B.; Monti, D.; Johansson, P.; Ponrouch, A., Cation Solvation and Physicochemical Properties of Ca Battery Electrolytes. *J. Phys. Chem. C* **2019**, *123*, 29524-29532.
27. Han, K. S.; Hahn, N. T.; Zavadil, K. R.; Jaegers, N. R.; Chen, Y.; Hu, J. Z.; Murugesan, V.; Mueller, K. T., Factors Influencing Preferential Anion Interactions During Solvation of Multivalent Cations in Ethereal Solvents. *J. Phys. Chem. C* **2021**, *125*, 6005–6012.
28. Shakourian-Fard, M.; Kamath, G.; Taimoory, S. M.; Trant, J. F., Calcium-Ion Batteries: Identifying Ideal Electrolytes for Next-Generation Energy Storage Using Computational Analysis. *J. Phys. Chem. C* **2019**, *123*, 15885-15896.
29. Araujo, R. B.; Thangavel, V.; Johansson, P., Towards Novel Calcium Battery Electrolytes by Efficient Computational Screening. *Energy Storage Mater* **2021**, *39*, 89-95.
30. Young, J.; Kulick, P. M.; Juran, T. R.; Smeu, M., Comparative Study of Ethylene Carbonate-Based Electrolyte Decomposition at Li, Ca, and Al Anode Interfaces. *ACS Appl. Energy Mater.* **2019**, *2*, 1676-1684.
31. Young, J.; Smeu, M., Ethylene Carbonate-Based Electrolyte Decomposition and Solid–Electrolyte Interphase Formation on Ca Metal Anodes. *J. Phys. Chem. Lett.* **2018**, *9*, 3295-3300.
32. Yang, F., et al., Probing Calcium Solvation by Xas, Md and Dft Calculations. *RSC Adv.* **2020**, *10*, 27315-27321.
33. Biria, S.; Pathreeker, S.; Genier, F. S.; Hosein, I. D., A Highly Conductive and Thermally Stable Ionic Liquid Gel Electrolyte for Calcium-Ion Batteries. *ACS Appl. Poly. Mater.* **2020**, *2*, 2111–2118.
34. Cabello, M.; Nacimiento, F.; Gonzalez, J. R.; Ortiz, G.; Alcantara, R.; Lavela, P.; Perez-Vicente, C.; Tirado, J. L., Advancing Towards a Veritable Calcium-Ion Battery: Caco2o4 Positive Electrode Material. *Electrochem. Commun.* **2016**, *67*, 59-64.
35. Kim, S., et al., High-Voltage Phosphate Cathodes for Rechargeable Ca-Ion Batteries. *ACS Energy Lett.* **2020**, *5*, 3203-3211.

36. Chae, M. S.; Kwak, H. H.; Hong, S. T., Calcium Molybdenum Bronze as a Stable High-Capacity Cathode Material for Calcium-Ion Batteries. *ACS Appl. Energy Mater.* **2020**, *3*, 5107-5112.
37. Park, H.; Cui, Y. J.; Kim, S.; Vaughey, J. T.; Zapol, P., Ca Cobaltites as Potential Cathode Materials for Rechargeable Ca-Ion Batteries: Theory and Experiment. *J. Phys. Chem. C* **2020**, *124*, 5902-5909.
38. Kresse, G.; Furthmüller, J., Efficient Iterative Schemes for Ab Initio Total-Energy Calculations Using a Plane-Wave Basis Set. *Phys Rev B* **1996**, *54*, 11169-11186.
39. Plimpton, S., Fast Parallel Algorithms for Short-Range Molecular-Dynamics. *J Comput Phys* **1995**, *117*, 1-19.
40. Crabb, E.; France-Lanord, A.; Leverick, G.; Stephens, R.; Shao-Horn, Y.; Grossman, J. C., Importance of Equilibration Method and Sampling for Ab Initio Molecular Dynamics Simulations of Solvent–Lithium-Salt Systems in Lithium-Oxygen Batteries. *Journal of Chemical Theory and Computation* **2020**, *16*, 7255-7266.
41. Melchionna, S.; Ciccotti, G.; Holian, B. L., Hoover Npt Dynamics for Systems Varying in Shape and Size. *Mol Phys* **1993**, *78*, 533-544.
42. Huang, Q. W.; Lourenco, T. C.; Costa, L. T.; Zhang, Y.; Maginn, E. J.; Gurkan, B., Solvation Structure and Dynamics of Li+ in Ternary Ionic Liquid-Lithium Salt Electrolytes. *J Phys Chem B* **2019**, *123*, 516-527.
43. Perdew, J. P.; Burke, K.; Ernzerhof, M., Generalized Gradient Approximation Made Simple. *Phys. Rev. Lett.* **1996**, *77*, 3865-3868.
44. Cheng, L.; Redfern, P.; Lau, K. C.; Assary, R. S.; Narayanan, B.; Curtiss, L. A., Computational Studies of Solubilities of Lio2 and Li2o2 in Aprotic Solvents. *J. Electrochem. Soc.* **2017**, *164*, E3696-E3701.
45. Asada, M.; Fujimori, T.; Fujii, K.; Kanzaki, R.; Umebayashi, Y.; Ishiguro, S.-i., Solvation Structure of Magnesium, Zinc, and Alkaline Earth Metal Ions in N,N-Dimethylformamide, N,N-Dimethylacetamide, and Their Mixtures Studied by Means of Raman Spectroscopy and Dft Calculations—Ionic Size and Electronic Effects on Steric Congestion. *J Raman Spectrosc* **2007**, *38*, 417-426.
46. Åvall, G.; Mindemark, J.; Brandell, D.; Johansson, P., Sodium-Ion Battery Electrolytes: Modeling and Simulations. *Adv. Energy Mater.* **2018**, *8*, 1703036.
47. Xu, K.; von Wald Cresce, A., Li+-Solvation/Desolvation Dictates Interphasial Processes on Graphitic Anode in Li Ion Cells. *J. Mater. Res.* **2012**, *27*, 2327-2341.
48. Okoshi, M.; Yamada, Y.; Yamada, A.; Nakai, H., Theoretical Analysis on De-Solvation of Lithium, Sodium, and Magnesium Cations to Organic Electrolyte Solvents. *J. Electrochem. Soc.* **2013**, *160*, A2160-A2165.
49. Yamijala, S. S. R. K. C.; Kwon, H.; Guo, J.; Wong, B. M., Stability of Calcium Ion Battery Electrolytes: Predictions from Ab Initio Molecular Dynamics Simulations. *ACS Appl. Mater. Interfaces* **2021**.
50. Tchitchekova, D. S.; Ponrouch, A.; Verrelli, R.; Broux, T.; Frontera, C.; Sorrentino, A.; Bardé, F.; Biskup, N.; Arroyo-de Dompablo, M. E.; Palacín, M. R., Electrochemical Intercalation of Calcium and Magnesium in Tis2: Fundamental Studies Related to Multivalent Battery Applications. *Chem. Mater.* **2018**, *30*, 847-856.
51. Wang, J.; Tan, S.; Xiong, F.; Yu, R.; Wu, P.; Cui, L.; An, Q., Vopo4·2h2o as a New Cathode Material for Rechargeable Ca-Ion Batteries. *Chem Commun* **2020**, *56*, 3805-3808.

TOC Graphic